



Pulsed laser deposited KNbO₃ thin films for applications in high frequency range

A. Rousseau, Vincent Laur, Maryline Guilloux-Viry, Gérard Tanné, Fabrice Huret, S. Députier, A. Perrin, F. Lalu, Paul Laurent

► To cite this version:

A. Rousseau, Vincent Laur, Maryline Guilloux-Viry, Gérard Tanné, Fabrice Huret, et al.. Pulsed laser deposited KNbO₃ thin films for applications in high frequency range. Thin Solid Films, 2006, 515, pp.2353-2360. 10.1016/j.tsf.2006.04.010 . in2p3-00128650

HAL Id: in2p3-00128650

<https://hal.in2p3.fr/in2p3-00128650>

Submitted on 8 Mar 2007

HAL is a multi-disciplinary open access archive for the deposit and dissemination of scientific research documents, whether they are published or not. The documents may come from teaching and research institutions in France or abroad, or from public or private research centers.

L'archive ouverte pluridisciplinaire **HAL**, est destinée au dépôt et à la diffusion de documents scientifiques de niveau recherche, publiés ou non, émanant des établissements d'enseignement et de recherche français ou étrangers, des laboratoires publics ou privés.

Pulsed laser deposited KNbO₃ thin films for applications in high frequency range

A. Rousseau¹, V. Laur², M. Guilloux-Viry^{1*}, G. Tanné², F. Huret², S. Députier¹, A. Perrin¹,
F. Lalu³ P. Laurent²

1- Institut de Chimie de Rennes, LCSIM - UMR 6511 CNRS/ University of Rennes 1,
35042 Rennes Cedex, France

2- LEST - UBO/ENSTBr –UMR CNRS 6165, 6, Av. Le Gorgeu, C.S. 93837, 29238
BREST cedex 3, France

3- CSNSM, Bât. 108, 91405 ORSAY CAMPUS, France

* Corresponding author. Tel: +33-2-23-23-56-55
E-mail address: maryline.guilloux@univ-rennes1.fr

PACS Codes : 77.55.+f, 77.84.Dy, 68.55.-a, 68.55.Nq, 81.15.Fg

Abstract

Potassium niobate thin films were grown by pulsed laser deposition on various substrates. Influence of deposition conditions on films characteristics was studied. Structural investigation evidenced that single phase polycrystalline randomly oriented films were grown on sintered alumina whereas epitaxial films were grown on (100)SrTiO₃ and (100)MgO substrates. The microstructure was highly controlled by the structural characteristics. Interdigitated capacitors built from KNbO₃ films on two different substrates (alumina and MgO) showed the strong influence of the structural characteristics on the dielectric behaviour. The variation of the equivalent capacitance measured on the interdigital capacitor on MgO was 6.4 % at 2.5 GHz while it was 1.5 % on alumina, in both cases for a moderate applied field of $\sim 15 \text{ kV.cm}^{-1}$. The results show the potentiality of this ferroelectric materials for use in frequency agile microwave electronics.

Key words: ferroelectric properties, structural properties, laser ablation, potassium niobate

Introduction

The evolution of telecommunication systems toward multistandard applications have motivated many studies to develop tunable circuits giving access to various functions together with different standards [1, 2].

Ferroelectrics are attractive materials for applications in electrically tunable high frequency devices [3]. Indeed ferroelectrics are characterized by non-linear dielectric properties [4] and then exhibit an electric field dependent dielectric permittivity (ϵ). Devices performances strongly depend on the ferroelectrics characteristics: Curie Temperature (T_c) which determines the use in the paraelectric or ferroelectric phase, permittivity (ϵ), and losses ($\tan\delta$). Implications of using materials in the paraelectric or ferroelectric state are still under discussion, depending on application [5]. The use of thin film offers several advantages over bulk materials for tunable microwave circuits such as lower bias voltages and potentiality for monolithic integration. Recent efforts have focused mainly on $\text{Ba}_x\text{Sr}_{1-x}\text{TiO}_3$ thin films [6, 7] because of its interesting compromise in terms of dielectric losses and agility. Among ferroelectrics, another family of materials, $\text{KTa}_{1-x}\text{Nb}_x\text{O}_3$ ($0 \leq x \leq 1$) could be also a promising candidate for the design and achievement of tunable devices. Indeed, as $\text{Ba}_x\text{Sr}_{1-x}\text{TiO}_3$, they are perovskite-like compounds well known as low loss materials [5, 8] for which T_c can be monitored by choosing a selected composition in the solid solution KTaO_3 - KNbO_3 [9]: the Curie temperature is expected to vary continuously according to the formula $T_c [\text{K}] = 676x + 32$ (for $x \geq 4.5 \%$) [9, 10]. Furthermore, $\text{KTa}_{1-x}\text{Nb}_x\text{O}_3$ thin films growth generally requires deposition temperatures about 100°C lower than those for $\text{Ba}_x\text{Sr}_{1-x}\text{TiO}_3$ materials with similar crystalline characteristics [6, 11].

In the present work, we studied KNbO_3 (abbreviated KN in the following) thin films for microwave tunable devices. KN is a ferroelectric material well known for its potentiality

of application in different areas because it has large electro-optic coefficient [12], nonlinear optical coefficient [13] and excellent photorefractive properties [14]. A previous study on dielectric properties of epitaxial KN showed promising agility of about 40% at low frequency up to 12 MHz under a dc-bias of 70 kV.cm^{-1} [15].

Thin film deposition of KN has been already reported in the literature using ion beam sputtering [16], metalorganic chemical vapor deposition [17, 18], sol gel method [19], rf sputtering [20] and pulsed-laser deposition (PLD) [21]. Control of KN thin films requires an optimization of deposition conditions essentially because of high volatility of potassium.

In this paper, we report on KN thin films grown by PLD on various substrates taking into account that low permittivity and low loss substrates are necessary for microwaves range. Moreover, orientation and microstructure of thin films are of first importance because of both anisotropic properties and losses which can be strongly affected by grain boundaries effects. Sintered alumina was chosen as a low cost substrate, routinely used in microwaves field, to determine the deposition conditions of KN. In order to compare polycrystalline non oriented films with epitaxial thin films grown on single crystal substrates, SrTiO_3 was selected as a model perovskite substrate for the study of growth conditions, in spite of its dielectric characteristics not suitable for microwave applications. Finally KN was deposited on MgO single crystal substrate which, in contrast, is suitable for the microwaves range.

Experimental procedure

1- Deposition

KN thin films were grown *in situ*, i.e. without any further treatment, by pulsed laser deposition using a KrF excimer laser (Tuilaser Excistar, pulse duration of 20 ns, $\lambda = 248 \text{ nm}$),

with a focused energy density of $\sim 1.5 \text{ J/cm}^2$, operating at 2 Hz. The laser beam, incident at 45° , was focused on the target which was rotated in a standard vacuum chamber (background pressure of about $5 \times 10^{-4} \text{ Pa}$).

Potassium niobate thin films were deposited from home-made sintered targets. KN targets were prepared by solid state reaction using a conventional sintering process. The KN powder was first synthesised from stoichiometric mixture of K_2CO_3 and Nb_2O_5 powders calcined in air at 1000°C for 12h. Then, cylindrical pellets, 25 mm in diameter, $\sim 5 \text{ mm}$ thick, were obtained by sintering KN at 350°C during 12 hours. This resulted in a quite dense target (typically compacity corresponds to 65-75% of KN theoretical density), the surface of which was polished before each deposition run. In order to compensate potassium loss during deposition, K-enriched targets were prepared by adding KNO_3 to the KN powders. These targets were liquid phase assisted sintered at 350°C for 12 hours. The thin films were grown in the temperature range $600^\circ\text{C} - 725^\circ\text{C}$, under an oxygen pressure ranging from 1 to 100 Pa and the substrate – target distance was fixed at 60 mm in order to obtain homogeneous films [21].

2- Characterization

The chemical composition of thin films was determined by energy dispersive X-ray spectroscopy (EDS) using a Link Oxford analyser implemented on a Jeol JSM-6400 scanning electron microscope (SEM) which gives also access to electron channeling patterns (ECP) [22], and by Rutherford backscattering spectroscopy (RBS). RBS experiments were performed on ARAMIS accelerator in Orsay [23], using a 2 MeV He^{2+} ion beam. The energy detector was positioned at a 165° scattering angle with respect to He^{2+} ion beam direction. EDS results on thin films are very sensitive to the analysis parameters. Therefore the EDS

analysis was calibrated from RBS spectra. A 10 kV accelerating voltage and 10 nA beam current were used to obtain a reliable composition in potassium and niobium. Thin films were coated with a graphite thin layer to limit charge effects.

The surface morphology of the thin films was observed with a field effect emission scanning electron microscope (FESEM, JEOL F-6301) operated at low voltage (typically 9 kV) in order to limit charge effects and to achieve a high resolution without the need of surface metallization.

Non oriented films grown on alumina were characterized by X-ray diffraction (XRD) using a diffractometer equipped with a curved position-sensitive detector (INEL CPS 120, Cu $K_{\alpha 1}$ radiation). Epitaxial films were analysed by XRD using a four-circle texture diffractometer (Bruker AXS D8 Discover) operated with Cu $K_{\alpha 1}$ radiation in θ -2 θ , ω -scan and ϕ -scan modes. In-plane ordering was qualitatively checked by electron channeling pattern (ECP).

Interdigital capacitors (IDCs) were processed in coplanar technology by depositing metallic electrode on the top of the KN thin films by screen-printing from a gold paste (Dupont de Nemours) and patterned by standard photolithography and etching by KI solution. Electrode thickness was 4 μm . Microwave measurements were carried out with a Wiltron 37369A network analyser and a probe station, in the frequency range 40 MHz – 40 GHz at room temperature, firstly with no applied voltage and then with an increasing electric potential up to a 30 V maximum voltage due to probe station limitations.

Results and discussion

1- Deposition parameters optimization

Firstly, we deposited KN on polished alumina substrates in order to determine the optimum deposition conditions. The first step was the control of stoichiometry of the film in spite of the loss of potassium which can occur during deposition because of potassium volatility. Effets of the deposition temperature, of the pressure and of the target composition were investigated. KN films were grown starting from a stoichiometric target under a dioxygen pressure fixed at $0.3 \cdot 10^2$ Pa, the temperature varying in the range 600°C - 725°C. It was reported that KN films deposited at a temperature lower than 600 °C were not or poorly crystallized [24]. The evolution of the thin films composition with deposition temperature is given in figure 1. It is worth noting that the K/Nb ratio is always lower than unity for all over the temperature range and that it decreases when the temperature increases as it can be expected for a non-stoichiometry due to potassium volatility. The analysis of further samples grown of a fixed the temperature of 650°C and pressure of dioxygen varied from 1 to 100 Pa showed that the K/Nb ratio increased when the pressure increased, reaching a maximum value of approximately 0.85 for pressures between 70 and 100 Pa of O₂, in agreement with results previously reported [25]. Various approaches can be explored to compensate such deficiency like the use of an enriched target or a sequential deposition process [26]. In the case of KN or KTa_{1-x}Nb_xO₃ some groups investigated deposition from potassium enriched targets in various configurations: either K enriched targets [21] or segmented targets [25].

We used two compositions of potassium enriched targets, namely with 25 % and 50 % mol excess of KNO₃. Thin films were subsequently deposited from these targets on alumina substrates. Deposition temperatures were fixed at 650°C, 675°C and 700°C, and the oxygen pressure at 30 Pa. The K/Nb ratio of these films, determined by EDS analysis, are given in figure 2; K/Nb ratio of thin films deposited from a stoichiometric target are reported for comparison. For the target containing a K excess of 25 %, stoichiometric films (K/Nb = 1) were achieved for deposition temperature of 650°C, whereas for higher temperature

potassium deficient films were obtained. In contrast, using a 50 % mol excess of potassium in the target gives access to stoichiometric films at 700°C.

Figure 3 shows the typical XRD patterns routinely obtained for films deposited from the various targets under various conditions. The first type of pattern (a) is characteristic of the thin films for which the K/Nb ratio is lower than 1. In this case, diffraction peaks are characteristic of KNbO_3 [27] with the presence of a secondary phase $\text{K}_4\text{Nb}_6\text{O}_{17}$ also mentioned by other groups [19, 28]. For the second type (b), relative to films having the correct stoichiometry ($\text{K/Nb} \sim 1$), the patterns are characteristic of single phase KN. Finally, the last type of pattern (c) is observed in the case of films deposited from a target doped with 50% mol excess of K at 650°C under an oxygen pressure of 30 Pa. The K/Nb ratio is then higher than 1, and the XRD pattern is characterized by the emergence of peaks of K_3NbO_4 (JCPDS 30-0964) additionally to those of KN. Then, we chose targets prepared with 50% K mol excess for deposition at 700 °C in order to improve crystallisation.

The deposition pressure was then optimized : figure 4 shows that stoichiometric films were achieved for 30 Pa, which was selected for the further experiments. 30 Pa was preferred to 40 Pa in order to avoid any slight excess of K which seems to be more deleterious than a very slight K deficiency. In fact a K excess can promote formation of moisture sensitive secondary phases. These conditions are close to those previously mentioned, however in comparison with other works performed with a unique K enriched target, we obtained stoichiometric films from 50 % mol excess K , which is lower than the 100 % excess which was reported [21].

2- Epitaxial films grown onto (100)-cut SrTiO_3 substrates

The above optimized conditions were used to grow epitaxial films on (100)SrTiO₃ single-crystal substrates (labelled STO in the following). STO presents a cubic structure at room temperature with a lattice constant of 3.905 Å and then is a standard substrate for the study of the epitaxial growth of perovskite compounds. KN exhibits a first-order ferroelectric phase transition accompanied by a change from cubic to tetragonal at 435 °C. Upon further cooling the structure changes from tetragonal to orthorhombic at 225 °C and to rhombohedral below -10°C [29, 30]. The lattice parameters of the orthorhombic unit cell of KN at room temperature are $a = 5.696$ Å, $b = 5.7213$ Å, $c = 3.9739$ Å. The lattice mismatch between the $\langle 100 \rangle$ directions of STO and the $\langle 110 \rangle$ directions of KN is $\sim 2\%$ at room temperature. It is $\sim 3\%$ at the growth temperature, considering the cubic cell.

Samples grown under the optimized growth conditions (700°C, 30 Pa of O₂, target with 50% excess K) as mentioned above, exhibit a high structural quality as attested by XRD pattern, evidencing the (110) orientation of the films (figure 5). The low value of $\Delta\omega = 0.2^\circ$ for the full width at half maximum (FWHM) of the ω -scan performed on the 110 peak is the signature of a low mosaicity effect.

The evolution of $\Delta\omega$ when varying the deposition temperature (figure 6) confirms that 700°C is an optimal value. In agreement with results reported by Chang *et al* [31] for KTa_{1-x}Nb_xO₃ films, increasing temperature above 725°C did not further improve the results.

The extremely sharp ECP (figure 7a) reveals the epitaxial growth of these films. The pseudo four-fold symmetry of the ECP is characteristic of the (hh0) orientation of KN taking into account the very close value of a and b unit-cell constants. This shows that KN grows in a cube on cube geometry on (100)STO substrates, when considering the pseudocubic perovskite sub-cell [17, 32]. Figure 7b depicts the typical morphology of films deposited on (100)STO substrates at a temperature ranging from 650°C to 725°C. It can be seen that the

(110) epitaxial growth of the as deposited films leads to a dense microstructure made of regular, ordered and square shaped grains with dimensions between 50 and 100 nm.

3- Epitaxial films grown onto (100)MgO substrates.

In view of microwaves applications KN thin films were deposited on (100)MgO substrates with experimental conditions given above. The substrates of MgO ($\epsilon_r = 9.6$, $\text{tg}\delta = 9 \times 10^{-4}$ at 300 K, 10 GHz) were selected because they are suitable for the microwaves range contrary to the substrates of STO ($\epsilon_r = 277$ et $\text{tg}\delta = 2 \times 10^{-2}$ at 300 K, 10 GHz), as well as for KN epitaxial growth. As MgO presents a cubic structure with a lattice constant of 4.213 Å at room temperature, the lattice mismatch between the $\langle 100 \rangle$ directions of MgO and the $\langle 110 \rangle$ directions of KN of $\sim 6\%$ is significantly higher than for STO. A typical θ -2 θ XRD pattern of KN films deposited at 700°C under 30 Pa of O₂, shown in figure 8, reveals only hh0 peaks of KN on (100)MgO. The FWHM of the ω -scan peaks range typically between 0.8° and 1.5°, that is larger than those at the films grown on the STO substrate, due to the larger mismatch in the case of MgO.

In spite of this mismatch, thin films grown on (100)MgO are epitaxial-like as shown by ϕ -scan XRD patterns (figure 9) performed on the 200 reflection of KN. The azimuthal coincidence of the reflections arising from {200} KN and {220} MgO planes implies that the in-plane directions [001] KN and [1-10] KN are aligned with the substrate axes, exactly as in the case of STO.

As expected, structural characteristics strongly influence the films morphology, as evidenced by scanning electron microscopy observation (figure 10). Indeed, the epitaxial films exhibit a quite dense and well organized in-plane microstructure, in agreement with the in-plane structural ordering. However, in contrast with STO, KN films grown on MgO

surfaces tend to develop with columnar-like structures, increasing their surface roughness. These columns have been attributed to the formation of $\text{Mg}(\text{OH})_2$ on the MgO surface which acts as nucleation centers [33]. Film composition and thickness were determined by RBS.

A typical RBS spectrum for a KN thin film deposited on MgO is reported in figure 11 : the K/Nb ratio is equal to 1.00 ± 0.05 and the thickness is approximately 160 nm for 20 minutes of deposition.

The film thickness was increased in order to built capacitors. In some cases KN/MgO films thicker than around $0.4 \mu\text{m}$ exhibited cracking after deposition as mentioned in [31]. This behaviour illustrates the presence of strain in the thin film which can be caused by several contributions : film-substrate lattice mismatch, structural defects in the film or at the film/substrate interface, phase transition in the film, or a difference of expansion factor between film and substrate. The room temperature lattice mismatch for KN films is $\sim -6 \%$ with MgO substrate resulting in a in-plane tensile strain (average experimental measurement of KN in-plane unit cell constant $\sim 5.73 \text{ \AA}$) in contrast with the lattice mismatch of $\sim +2 \%$ with STO substrate (average experimental measurement of KN in-plane unit cell constant $\sim 5.70 \text{ \AA}$), which results in a compressive strain. According to Derderian et al. [19], potassium-rich films exhibit cracking. However, in our case, RBS analysis did not reveal any significant potassium excess in films. In order to decrease cracks formation, we increased cooling time. Indeed, an increase up to 6 hours resulted in crack-free films, supporting the hypothesis of cracks due to strain effect. Increasing the cooling time did not modify the structural characteristics.

High frequency behaviour

The objective of following circuits is to evaluate the potentialities of KN material for microwaves applications. Coplanar technology was chosen because, with respect to microstrip, it increases interactions between the ferroelectric thin film and the microwave field, and this technology does not require the presence of bottom electrode. Moreover, this geometry enables to achieve the same impedance with different slot and feed line widths. Thus, as the variation of permittivity is proportional to the amplitude of the applied electrical field, a wide or narrow range of variations can be selected. Here, we chose wide slots for access lines in order to limit impedance mismatch and narrow ones for capacitor fingers to provide a large tunability. Figure 12 shows the resulting heterostructures. Capacitors are formed with three pairs of fingers of 250 μm length with a gap (g) of 20 μm .

Moreover, in order to evaluate the influence of structural characteristics of the films on the high frequency dielectric behavior, coplanar interdigitated capacitors (IDCs) were realized on ~ 500 nm thick KN films epitaxially grown either on (100) MgO or on 500 nm thick films grown without any preferential orientation on sintered Al_2O_3 . Figure 13 displays the measured response between 20 MHz and 5 GHz for KN deposited on MgO substrates, without any applied voltage and with an applied dc bias of 15 V and 30 V.

The variation observed by voltage application remains about the same between 20 MHz and 5 GHz. The capacitance was determined from standard method with ADS program. Capacitance decreased from 0.346 pF to 0.324 pF when applied bias voltage was increased from 0 to $U_{\text{max}} = 30\text{V}$. The field-strength dependant tunability is obtained by :

$$\frac{\Delta C}{C} = \frac{[C(0\text{ V}) - C(30\text{ V})]}{C(0\text{ V})} \text{ for IDCs. The applied electric field (E) can be estimated to about}$$

$$15 \text{ kV.cm}^{-1} \text{ for } 30 \text{ V } (E \approx \frac{U_{\text{max}}}{g}), \text{ if we consider a homogenous in-plane distribution of the}$$

electric field. A variation of 6.4% on equivalent capacitance was obtained at 2.5 GHz (Figure 13) from this equation. In spite of the low amplitude of the applied field (15 kV.cm^{-1}), these

results are closely comparable with those obtained for BST materials with the same applied field [7]. The same coplanar capacitor processed on KN on alumina gives a variation of only 1.5% at 2.5 GHz. This result illustrates the influence of the epitaxial growth, associated with a dense and well ordered microstructure achieved on MgO (figure 10).

Moreover, ferroelectric behaviour of KNbO_3 at room temperature ($T_c = 708 \text{ K}$) involves remanence phenomena. Thus, successive measurements of this capacity showed a gradual reduction in the variation of the equivalent capacity. After some dc-voltage cycles, the equivalent capacity value of IDCs on MgO substrates decreased from 0.346 pF to 0.331 pF. To avoid this irreversibility effect, the next step will concern new materials belonging to the solid solution $\text{KTaO}_3 - \text{KNbO}_3$ called $\text{KTa}_{1-x}\text{Nb}_x\text{O}_3$ with $x \neq 1$ in which the Curie temperature (T_c) and then permittivity (ϵ), and losses ($\text{tg}\delta$) can be tuned by the control of composition (x).

Conclusions

Polycrystalline randomly oriented KN films on sintered alumina, and epitaxial films on (100)STO and on (100)MgO substrates were grown by PLD. High quality films were achieved provided that deposition parameters were systematically optimized. Stoichiometric films were obtained with deposition temperature of 700°C under 30 Pa of O_2 from a KN target to which an excess of 50% mol K was added. Coplanar interdigital capacitors were built on KN thin films grown on alumina and MgO substrates. Measurements of capacitance variations of these circuits were performed between 20 MHz and 5 GHz, firstly with no applied voltage and then in increasing electric potential up to a 30 V maximum voltage. The influence of the structural characteristics on the behaviour in microwave range was evidenced by the tunability measured on the film on MgO (6.4%) and on the film on alumina (1.5%), determined from the equivalent capacitance at the same frequency (2.5 GHz).

Despite the remanence phenomena of KN material, these first results of tunability in the microwaves range applying a moderate electric field ($\sim 15 \text{ kV.cm}^{-1}$) are promising for potentialities of this family of material. Indeed, taking into account the high Curie temperature, the variations measured for KN enable to foresee an interesting agility for $\text{KTa}_{1-x}\text{Nb}_x\text{O}_3$ materials designed to have a Curie temperature closer to ambient temperature and thus to expect stronger variations on their permittivity.

Acknowledgments

This work was supported by Region Bretagne under contract CACET n° A2CA33. Scanning electron microscopy was performed at CMEBA in University of Rennes 1. B. Della, G. Chuiton and R. Jezequel (LEST) are warmly acknowledged for circuits preparation. X-Ray Diffraction equipment was financially supported by French Ministry of Research, Région Bretagne, Ille et Vilaine district and Rennes Metropole (PPF, CPER).

References

- [1] G.M. Rebeiz, G.L. Tan, J.S. Hayden, IEEE Microwave Mag. 3 (2002) 72.
- [2] D.E. Oates; A. Piqué, K.S. Harshovardhan, J. Moses, G. Yang, G.F. Dionne, IEEE Trans. App. Supercond. 7 (1997) 2338.
- [3] M.J. Lancaster, J. Powell, A. Porch, Supercond. Sci. Technol. 11 (1998) 1323.
- [4] M. Maglione, U.T. Höchli, J. Joffrin, Phys. Rev. Lett. 57 (1986) 436.
- [5] S.S. Gevorgian, IEEE Transactions on microwave theory and techniques 49 (2001) 2117.
- [6] S.E. Moon, E.-K. Kim, M.-H. Kwak, H.-C. Ryu, Y.-T. Kim, K.-Y. Kang, S.-J. Lee, Appl. Phys. Lett. 83 (2003) 2166.
- [7] S.E. Moon, E.-K. Kim, M.-H. Kwak, H.-C. Ryu, Y.-T. Kim, K.-Y. Kang, S.-J. Lee, Appl. Phys. Lett., 83 (2003) 2166.
- [8] J. L. Davis, L.G. Rubin, J. Appl. Phys. 24 (1953) 1195.
- [9] S. Triebwasser, Phys. Rev. 114 (1959) 63.
- [10] D. Rytz, H. J. Scheel, J. Cristal Growth 59 (1982) 468.
- [11] T. Delage, C. Champeaux, A. Catherinot, J.F. Seaux, V. Mandrangeas, D. Cros, Thin Solid films 453-454 (2004) 279.
- [12] P. Günter, Opt. Commun 11 (1974) 285.
- [13] Y. Uematsu, Jpn. J. Appl. Phys. 13 (1974) 1362.
- [14] P. Günter, Phys. Rep. 93 (1982) 199.
- [15] S. Chattopadhyay, B.M. Nichols, J.-H. Hwang, T.O. Mason, B.W. Wessels, J. Mater. Res. 17 (2002) 275.
- [16] T.M. Graettinger, P.A. Morris, A. Roshko, A.I. Kingon, O. Auciello, D.J. Lichtenwalner, A.F. Chow, Mat. Res. Soc. Symp. Proc. 341 (1994) 265.
- [17] M.V. Romanov, I.E. Korsakov, A.R. Kaul, S.Y. Stefanovich, I.A. Bolshazkov, G. Wahl, Chem. Vap. Deposition 10 (2004) 318.

- [18] A. Onoe, A. Yoshida, K. Chikuma, Appl. Phys. Lett. 69 (1996) 167.
- [19] G.J. Derderian, J.D. Barrie, K.A. Aitchison, P.M. Adams, M.L. Mecartney, J. Am. Ceram. Soc. 77 (1994) 820.
- [20] S. Schowyn Thöny, H.W. Lehmann, P. Günter, Appl. Phys. Lett. 61 (1992) 373.
- [21] C. Zaldo, D.S. Gill, R.W. Eason, J. Mendiola, P.J. Chandler, Appl. Phys. Lett. 65 (1994) 502.
- [22] A. Perrin, M. Guilloux-Viry, C. Thivet, J.-C. Jegaden, M. Sergent, J. Le lannic, Jeol News 30E (1992) 26.
- [23] E. Cottureau, J. Chaumont, R. Meunier, H. Bernas, Nucl. Inst. and Meth., 45 (1990) 223.
- [24] R.F. Xiao, H.D. Sun, H.S. Siu, Y.Y. Zhu, P. Yu, G.K.L. Wong, Appl. Phys. Lett., 70 (1997) 164.
- [25] S. Yilmaz, T. Venkatesan, R. Gerhard-Multhaupt, Appl. Phys. Lett. 58 (1991) 2479.
- [26] S.M. Zanetti, J.R. Duclere, M. Guilloux-Viry, V. Bouquet, E.R. Leite, E. Longo, J.A. Varela, A.Perrin, J. Euro. Ceram. Soc. 21 (2001) 2199.
- [27] JCPDS-International Centre for Diffraction Data, PCPDFWIN, 1999, Card 32-0822
- [28] W.L. Suchanek, Chem. Mater. 16 (2004) 1083.
- [29] B.P. Matthias, J.P. Remeika, Phys. Rev. 82 (1951) 727.
- [30] G. Shirane, H. Danner, A. Pavlovic, R. Pepinsky, Phys. Rev. 1954, 93 (1954) 672.
- [31] W. Chang, A.C. Carter, J.S. Horwitz, S.W. Kirchoefer, J.M. Pond, K.S. Grabowski, D.B. Chrisey, Mat. Res. Soc. Symp. Proc. 493 (1998) 353.
- [32] V. Golapan, R. Raj, J. Appl. Phys. 81 (1997) 865.
- [33] A.F. Chow, D.J. Lichtenwalner, R.R. Woolcott, T.M. Graettinger, O. Auciello, A.I. Kingon, Appl. Phys. Lett. 65 (1994) 1073.

Figure Captions

Figure 1 : K/Nb ratio in KNbO_3 films versus deposition temperature. Deposition was performed from a stoichiometric target under an oxygen pressure of 30 Pa. The curve is a guide to the eyes.

Figure 2 : K/Nb ratio in KNbO_3 films versus deposition temperature for different targets compositions. Oxygen pressure was fixed at 30 Pa during deposition. The curves are guides to the eyes.

Figure 3 : XRD patterns of KNbO_3 thin films grown onto alumina : (a) potassium deficient films ; (b) stoichiometric films ; (c) potassium over stoichiometric films. Indexed peaks refer to the KNbO_3 phase. Peaks marked as (#), (+) and (*) correspond to the substrate, to $\text{K}_4\text{Nb}_6\text{O}_{17}$ and to K_3NbO_4 respectively.

Figure 4 : K/Nb ratio in KNbO_3 films grown at 700°C versus oxygen pressure using a target prepared with 50% mol excess of KNO_3 . The curve is the guide to the eyes.

Figure 5 : θ -2 θ XRD pattern and rocking curve (KN (110) reflection) of KNbO_3 films on (100)STO substrates deposited at 700°C and 0.3 mbar O_2 .

Figure 6 : Variation of $\Delta\theta$ versus deposition temperature for KNbO_3 on (100)STO substrates.

Figure 7 : (a) ECP image of (110)KN films 160 nm thick epitaxially grown onto (100)STO and (b) FE-SEM image of the same film.

Figure 8 : θ -2 θ XRD pattern of KN films deposited on (100)MgO substrates at 700°C and 30 Pa of O_2

Figure 9 : XRD patterns in ϕ scan mode performed on the 200 reflection of KN (a) and on the 220 reflection of MgO (b). KN was deposited on (100)MgO at 700°C and 30 Pa of O_2 .

Figure 10 : Films morphology observed by scanning electron microscopy (a) KN on MgO, (b) KN on Al₂O₃. Magnification is the same in both cases (–: 100nm).

Figure 11 : RBS spectra of a stoichiometric (K/Nb = 1) KN film deposited at 700°C on (100)MgO.

Figure 12 : (a) Schematic cross section of the heterostructure, (b) Photograph of the coplanar interdigitated capacitors on ~ 500 nm thick KN films.

Figure 13 : DC-bias responses of IDC made from KNbO₃.

Figure 1

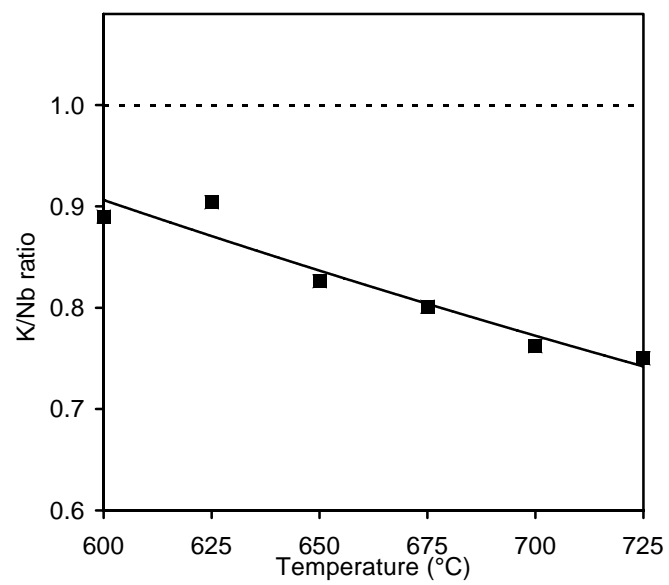


Figure 2

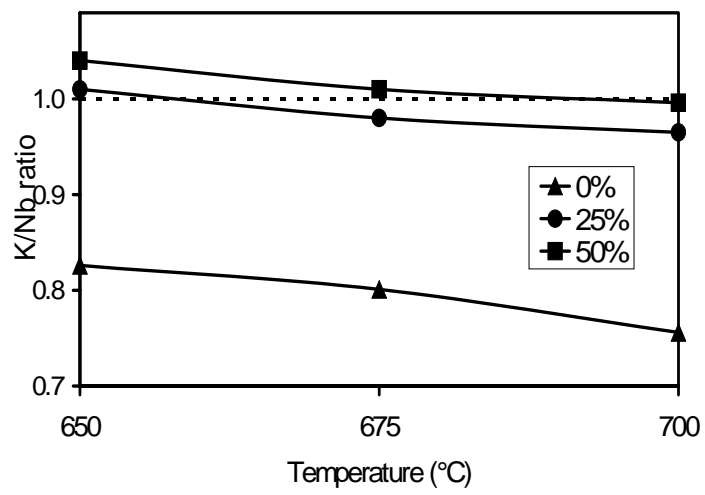


Figure 3

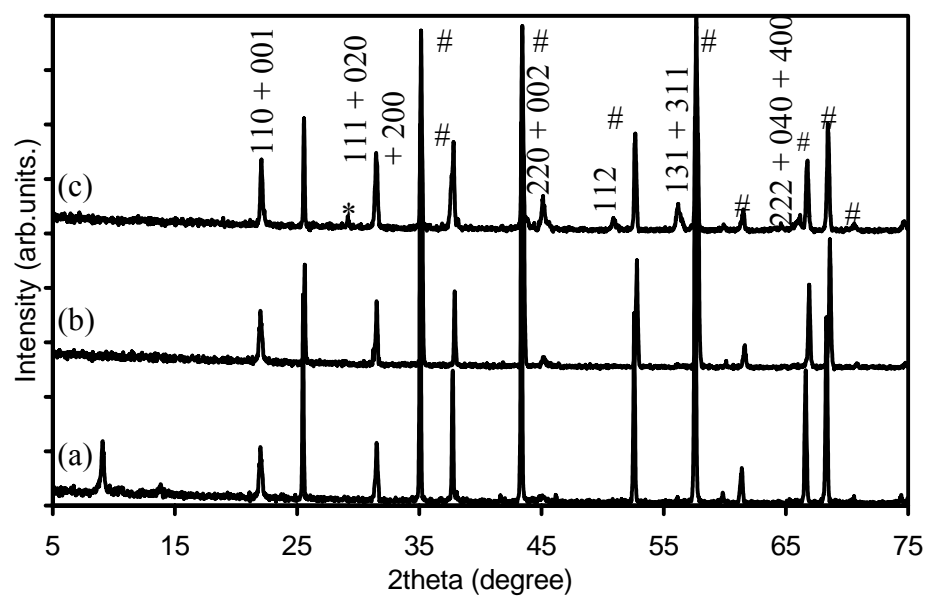


Figure 4

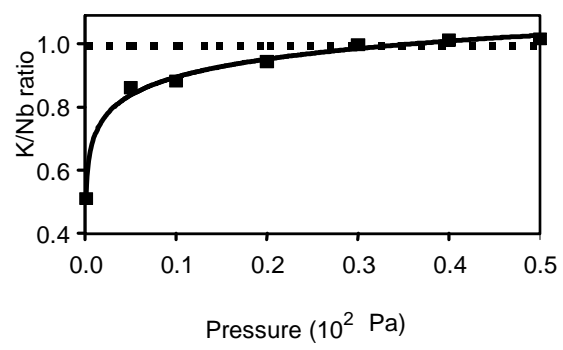


Figure 5

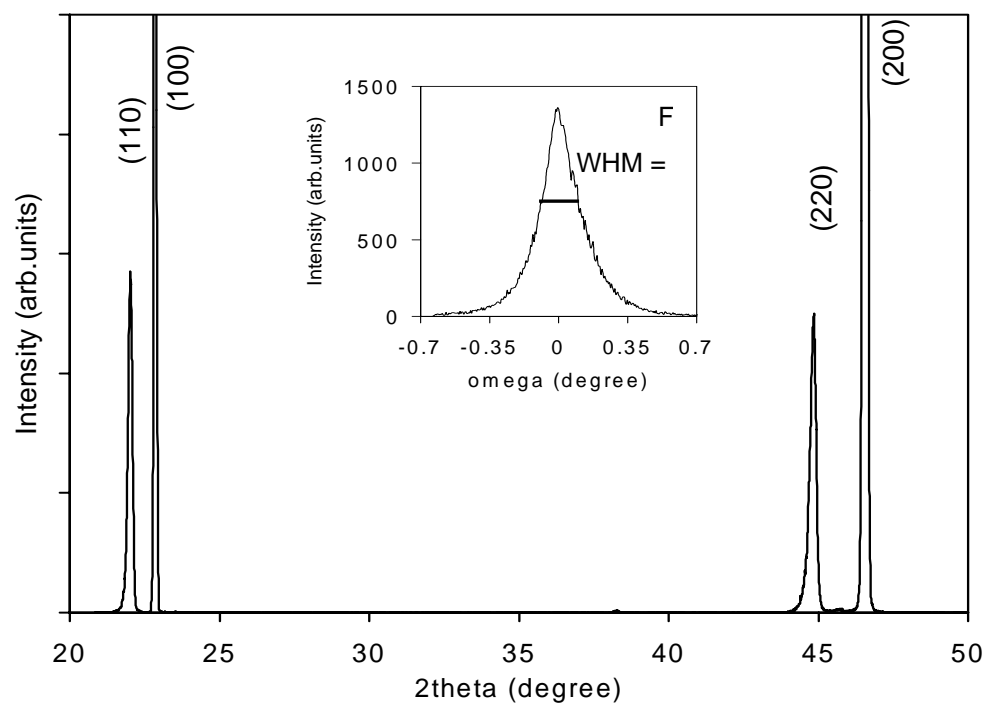


Figure 6

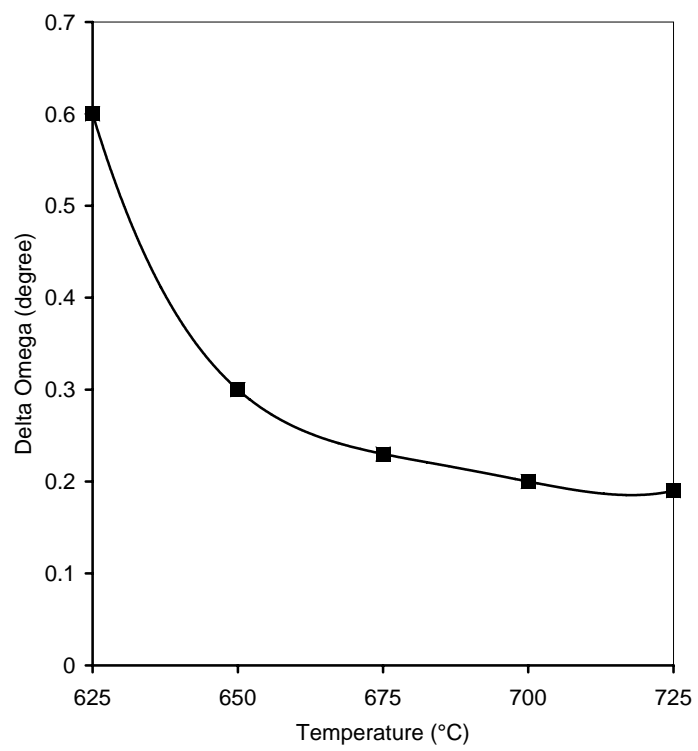


Figure 7

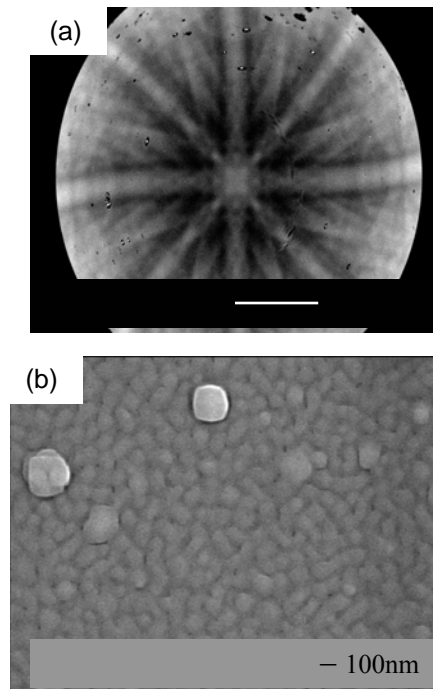


Figure 8

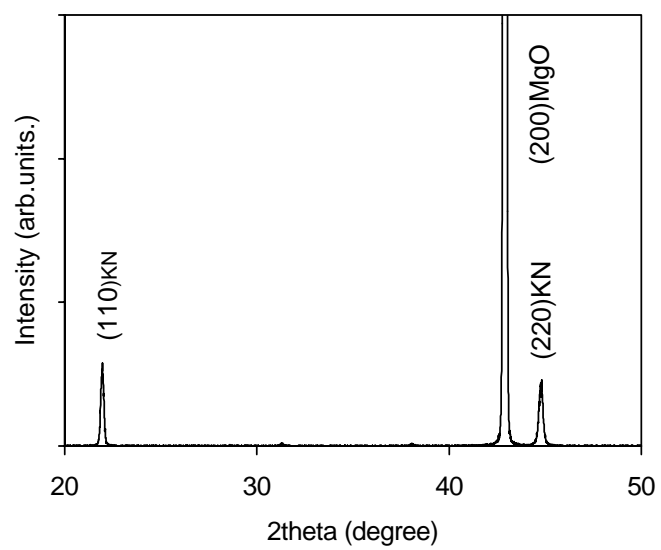


Figure 9

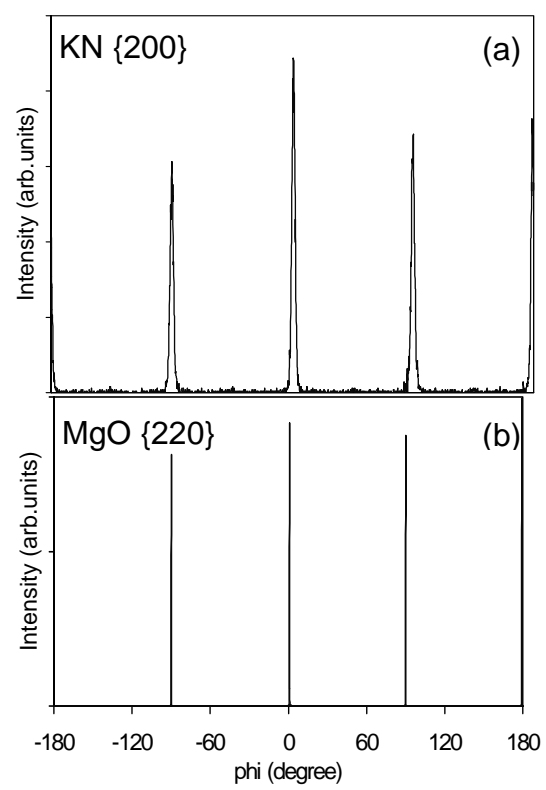


Figure 10

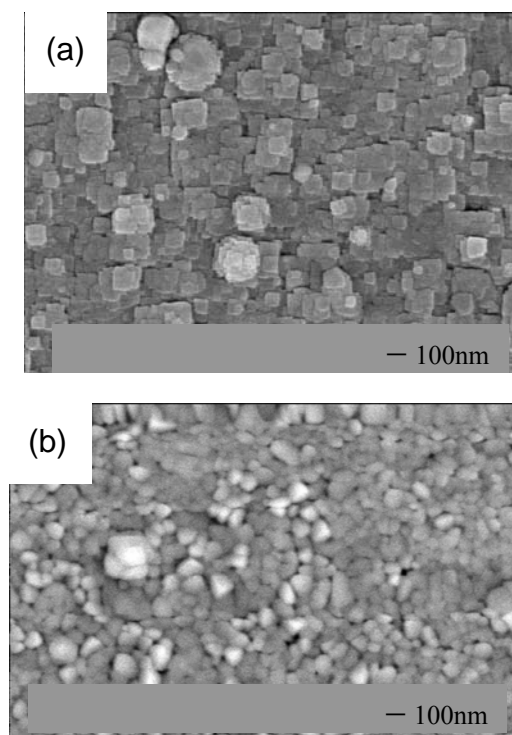


Figure 11

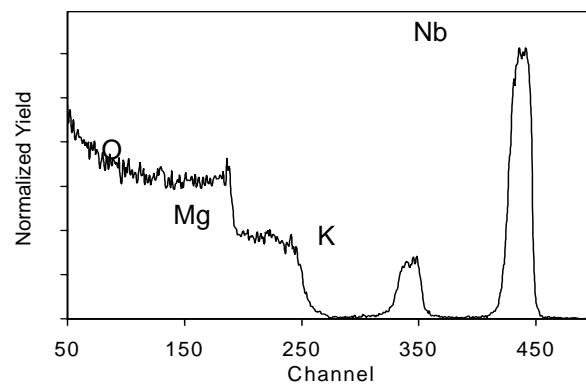


Figure 12

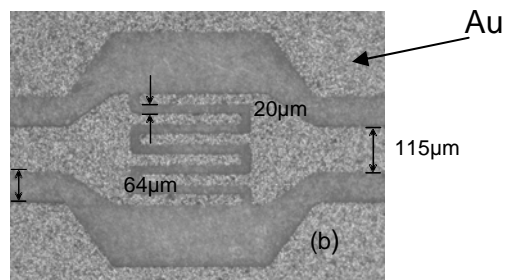
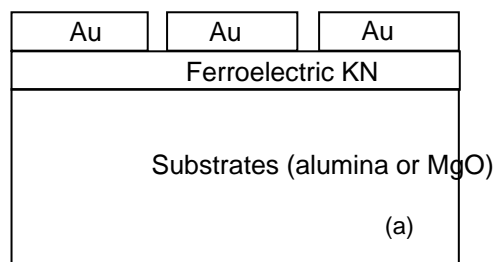


Figure 13

